

# Heights of formation of Fe I photospheric lines

A. Kučera<sup>1</sup>, H. Balthasar<sup>2,\*</sup>, J. Rybák<sup>1</sup>, and H. Wöhl<sup>2</sup>

<sup>1</sup> Astronomical Institute, Slovak Academy of Sciences, SK-05960 Tatranská Lomnica, Slovakia

<sup>2</sup> Kiepenheuer-Institut für Sonnenphysik, Schöneckstr. 6, D-79104 Freiburg, Germany

Received 9 April 1997 / Accepted 12 December 1997

**Abstract.** The determination of the location of spectral line-forming layers by means of line-depression contribution functions is checked by observational tests. The method is based on the assumption that the Doppler velocities derived from line bisectors at a given position in the profile of a spectral line are related to the actual bulk velocity at a particular height in the atmosphere. For a set of six magnetically sensitive and non-sensitive Fe I lines (543.45, 557.61, 630.15, 630.25, 649.50, 649.45 nm) the fluctuations of Doppler velocities along the slit of the spectrograph were determined at various  $\Delta\lambda$  from the line centers i.e. at various heights in the photosphere. Correlations of fluctuations allow us to find those parts in line profiles which are formed at identical heights in the photosphere. These experimental results are compared with theoretical estimates based on line depression contribution functions. The agreement is good and best results are found for nonmagnetic strong, but still unsaturated lines. The results support the hypothesis that it is possible to ascribe a single height point in the solar atmosphere to a given position in a spectral line profile.

**Key words:** sun: photosphere – sun: granulation – spectral line: profiles

## 1. Introduction

Photospheric spectral lines are generally used in order to probe the solar atmospheric layers in which they are formed. The question where the lines are formed exactly is therefore very important. In principle two approaches are published in the literature how to solve the described problem using a “Response function” (RF) or a “Contribution function” (CF). The RF is designed to predict the sensitivity of a line to a perturbation at a given depth. But that function does not tell us where the line is formed. The later information should be derived from CF. Magain (1986) developed selection criteria for both of these functions and proposed a convincing procedure to derive a rigorous expression for the *line depression contribution function* (LDCF) which should give us the relative contribution of the different atmospheric

layers to the observed quantity. A controversial literature exists on the subject, (e.g. Mein, 1971; Gurtovenko et al., 1974; Beckers & Milkey, 1975; Caccin et al., 1977; Makita, 1977, Sánchez et al. 1996). The RF can be quite different according to the line characteristics (e.g. Caccin et al. 1977). Therefore Sánchez et al. (1996) recently introduced a new concept to estimate heights in the atmosphere. They use RF but suggest to deal with *height of formation to measurement*. They argue that heights of formation should not be assigned to a single spectral line, since a single line may sample very different layers of the atmosphere, depending on the physical parameter of interest and the technique employed to determine it. (They concentrate on polarization induced by the magnetic field.) Concerning the magnetic atmosphere, Grossmann-Doerth et al. (1988) developed a suitable code for the computation of LDCF and RF for Stokes profiles. In a recent work Grossmann-Doerth (1994) used the code to determine the dependence of the LDCF of spectral lines on some relevant line parameters in the solar photosphere for the non-magnetic case. For the strong lines the author concluded that it is allowed to ascribe a rather narrow height range in the atmosphere to a given position in the line profile.

In the present paper we develop a method which can be used to test the above mentioned theoretical conclusions. The method is based on the investigation of fluctuations of some physical quantity along the spectrograph slit. We use the code from Grossmann-Doerth (1994) to compute the LDCF for theoretical verification of the experimental results. We deal with LDCFs instead of RFs, because the determination of the height of line formation is of our interest.

## 2. Method

We regard two spectral lines A and B (see Fig. 1) and assume that the center of line A is formed deeper in the solar atmosphere than the center of the second line. At a specific height of the solar atmosphere only one value of an appropriate physical parameter (i.e. velocity, magnetic field, pressure etc.) can exist. Thus, if we determine the fluctuations of any specific physical quantity along the spectrograph slit in the center of line A, identical fluctuations must definitely exist for some particular point (or a range) in profile B, because the center of line B is formed higher in the atmosphere than that of line A, and the wings of the

Send offprint requests to: A. Kučera (e-mail: akucera@ta3.sk)

\* Present address: Astrophysikalisches Institut Potsdam, Telegrafenberg, D-14473 Potsdam, Germany

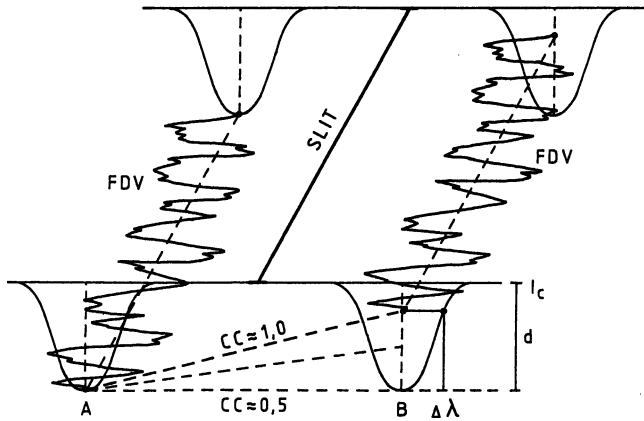


**Fig. 1.** The basic scheme of the suggested method. FDV = Fluctuations of the Doppler Velocity along the slit, A and B stay for spectral line A and B, respectively,  $I_c$  = continuum intensity,  $d$  = line depression, CC = correlation coefficient,  $\Delta\lambda$  = wavelength displacement with respect to wavelength of line center. See text in Sect. 2 for details.

B line are formed deep in the photosphere. Therefore, the height where the center of the line A is formed must unambiguously lay somewhere between these two extremes. Espagnet et al. (1995) found that the velocity fluctuations associated with the granulation cross the whole thickness of the photosphere. Therefore we used the “fluctuations of the Doppler velocity along the slit” (FDV) (see Fig. 1) to test our method. We are looking for a correlation of the FDV in the center of line A with the FDVs belonged to specific positions in line B. The correlation coefficient (CC) estimated for the line centers will be small because they are formed at different heights in the photosphere (in Fig. 1 this is assigned as  $CC = 0.5$ ), but somewhere at  $\Delta\lambda$  in the B profile the CC will be very high (in Fig. 1 this point is marked with  $CC = 1.0$ ). Finding the maximum of CC we can conclude that those two points which belonged to the center of line A and to the wing of line B are formed at identical heights in the solar atmosphere. This idealized assumption has limitations, which will be discussed in Sect. 6.

### 3. Observations and reductions

The observations were carried out with the Vacuum Tower Telescope at the Observatorio del Teide, Tenerife, on June 21, 1992. The Echelle spectrograph was used to take spectra in four spectral regions.

Here we only point out two important features: the resolution power of the spectrograph is better than  $6 \cdot 10^5$  and the spectral stray light is about 1%. The main characteristics of 5 spectral lines as well as the description of the observations were presented by Kučera et al. (1995). Here the same numbers are assigned to the lines (I to V for 543.45, 649.50, 630.15, 557.61, 630.25 nm, respectively). In addition we use a sixth Fe I line (VI at 649.45 nm). All four spectral regions were recorded strictly simultaneously (i.e. the same time of exposure = 10:26:52 UT, and with identical exposure times = 0.3 s) on four CCD cameras with 1024 x 1024 pixels each. The images were recorded

with  $2 \times 2$  binning mode with a pixel size of  $38 \mu$  squared. The width of the entrance slit was  $60 \mu$ . For the present work we have selected the best set which covers a region near the solar disk center. Only a purely quiet region inside a supergranule was selected for the investigation. It covers 45 arcseconds on the spectrograph slit.

The standard reduction of CCD images was performed using IDL and the Kiepenheuer Institute Library procedures. We follow the way described by Kučera et al. (1995). The positions of the spectral line centers show a trend along the slit. In order to determine this trend the telluric lines (630.20, 630.28 and 649.59 nm) were used as a reference. For the other two spectral regions (543.4 and 557.6 nm) we computed the trend using averaged images of these regions (flatfield source).

In order to determine the spectral line characteristics (continuum intensity  $I_c$ , line depression  $d$ , Doppler velocity at the line center  $D_v$ , and bisector Doppler velocities  $v_D$ ), the nearby local continuum for every scan was strictly used as an intensity reference. The bisector Doppler velocity definition is as follows: Let  $\lambda_0$  be the wavelength of the line center. For a given depression  $d$  we denote by  $\Delta\lambda_b$  and  $\Delta\lambda_r$  the wavelength displacement of the blue and the red wing position  $d(\Delta\lambda)$  with respect to  $\lambda_0$ . The bisector Doppler velocity  $v_D$  is then defined by

$$v_D(d) = 0.5(\Delta\lambda_b + \Delta\lambda_r)c/\lambda_0$$

where  $c$  is the velocity of light.

### 4. Experimental results

In all 6 lines the bisector Doppler velocities ( $v_D$ ) were used for constructions of FDVs at different intensity points of line depression, i.e. at different wavelength displacement  $\Delta\lambda$ . These displacements were selected appropriately in the line profiles to cover optimally the shape of the line (see asterisks in Fig. 3). The FDVs for the deepest and the highest formed lines (VI and I) are shown in Fig. 2.

The FDV in the center of line VI (the full thick line F in the first panel in Fig. 2) was correlated with the FDV in the center of the line I (the full thick line A in the second panel in Fig. 2). Thus, we obtained correlation coefficient  $c_0$ . The other correlation coefficients  $c_i$  ( $i=1,2,\dots,n$ ;  $n$  = number of specific positions in the profile of the line I) resulted from correlation of the FDV in the center of the line VI with the FDVs correspondent to the specific positions in the profile of the line I. The distribution of the  $c_0, c_1, c_2, \dots, c_n$  we named as  $C_{obs}$  (see diamonds in Fig. 3). An identical procedure was applied to all possible pairs of lines. In Table 1 we summarize the  $c_0$  for the line centers and the maximal value of  $c_i$  at  $\Delta\lambda$  obtained for the center of the first line and for an  $i$ -th specific position in the second line. The displacement  $\Delta\lambda$  for the appropriate  $i$ -th wing point is also added in Table 1.

Several facts can be extracted from Table 1:

There are identical values in the 4-th and 5-th columns for the lines IV and III. It means that the highest  $c_i$  occurs for the centers of these lines, i.e. they are really formed at identical heights in the photosphere. Very similar values appear for the lines II and I which are also formed at similar heights in the photosphere.

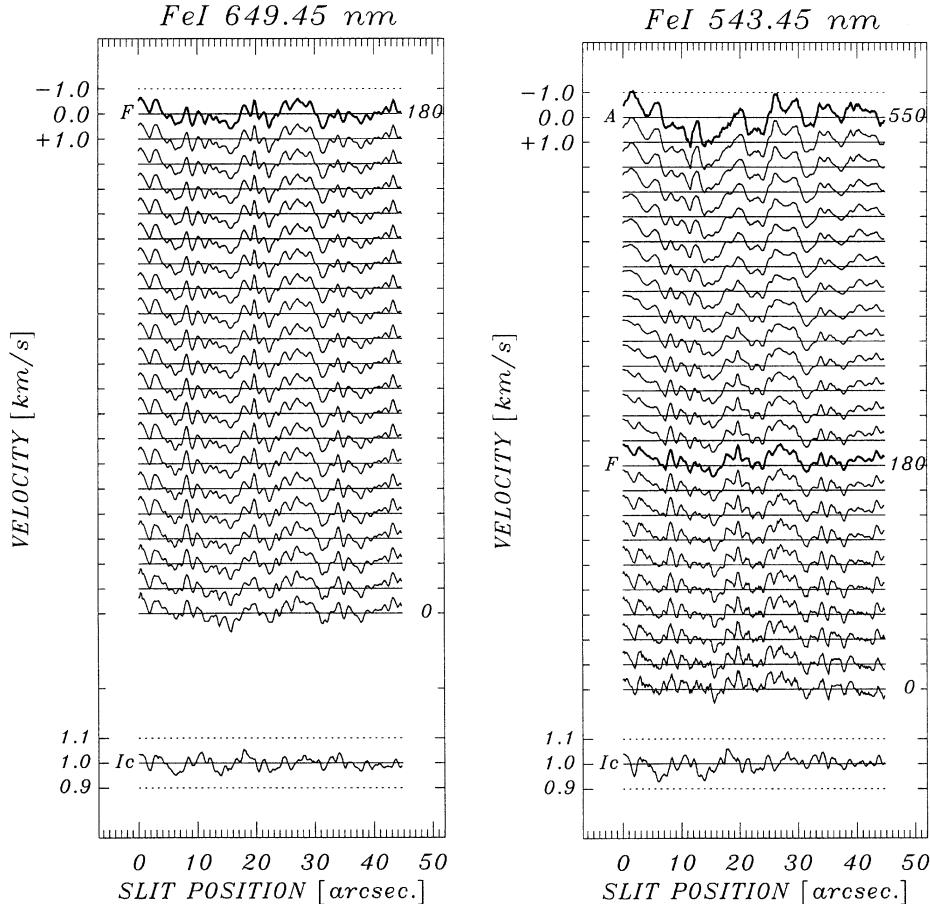


**Fig. 2.** The FDVs determined for lines VI and I. The scale is  $\pm 1$  km/s per track. The FDVs are given for successive intensity points in the line depression. The upper thick full line F (A) in the first (second) panel represents the FDVs in the center of line VI (I). The thick full line F in the second panel shows the FDV in the wing of line I which has the best correlation with the FDV in the center of line VI. The continuum intensity fluctuations along the slit ( $I_c$ ) are given at the bottom for comparison. The approximate height scale in km is assigned on the right side of the panels.

**Table 1.** Correlation coefficients  $c_0$ ,  $c_i$  for all line pairs. The formation heights of the line centers given stem from the line computation programs mentioned in Sect. 5. The heights are determined as the positions of the maxima of the LDCF computed for  $\lambda_o$ .

N	line pair	heights [km]	$c_0$	$c_i$ at $\Delta\lambda$	$\Delta\lambda$ [pm]
1	VI,I	180,550	0.545	0.919	8.9
2	VI,II	180,500	0.617	0.963	9.6
3	VI,III	180,340	0.846	0.972	7.4
4	VI,IV	180,310	0.802	0.957	6.3
5	VI,V	180,250	0.931	0.980	6.3
6	V,I	250,550	0.703	0.954	6.2
7	V,II	250,500	0.783	0.977	6.6
8	V,III	250,340	0.963	0.987	4.6
9	V,IV	250,310	0.940	0.981	4.5
10	IV,I	310,550	0.833	0.965	5.0
11	IV,II	310,500	0.891	0.970	5.0
12	IV,III	310,340	0.982	0.982	1.3
13	III,I	340,550	0.801	0.957	5.3
14	III,II	340,500	0.885	0.980	5.4
15	II,I	500,550	0.930	0.953	3.1

The maximal differences between columns 4 and 5 occur for the line pairs VI,I and VI,II, as expected. The maximal values of  $\Delta\lambda$  in the last column are found for the line pairs VI,I and VI,II, which show the maximal differences in the height of formation in the solar atmosphere for our lines.

The behaviour of the  $C_{obs}$  for the pairs of VI,I; V,I; IV,I and II, I lines are given in Fig. 3 together with the profiles of the lines.

## 5. Theoretical results

The experimental results gave us for every pair of lines the  $\Delta\lambda$  in the second line profile where the FDV has maximal correlation with the central FDV of the first line. Thus we have the chance to probe these experimental results theoretically by using LDCFs as sensitive indicators resulting from modeling. We used the computational code of Grossmann-Doerth (1994).

We use realistic photospheric models, one for the observed granular mean profile and another for the observed intergranular mean profile. These models are derived from the photospheric model T93-27 from Schleicher (1976) which is a modification of that from Holweger & Müller (1974). We changed the temperature around  $\lg \tau = 0$  by  $\pm 150$  K with a gaussian envelope. Additionally we reduce the temperature in the upper layers of the granular model by 100 K; this is justified by the results of Balthasar et al. (1990). The granular and intergranular models

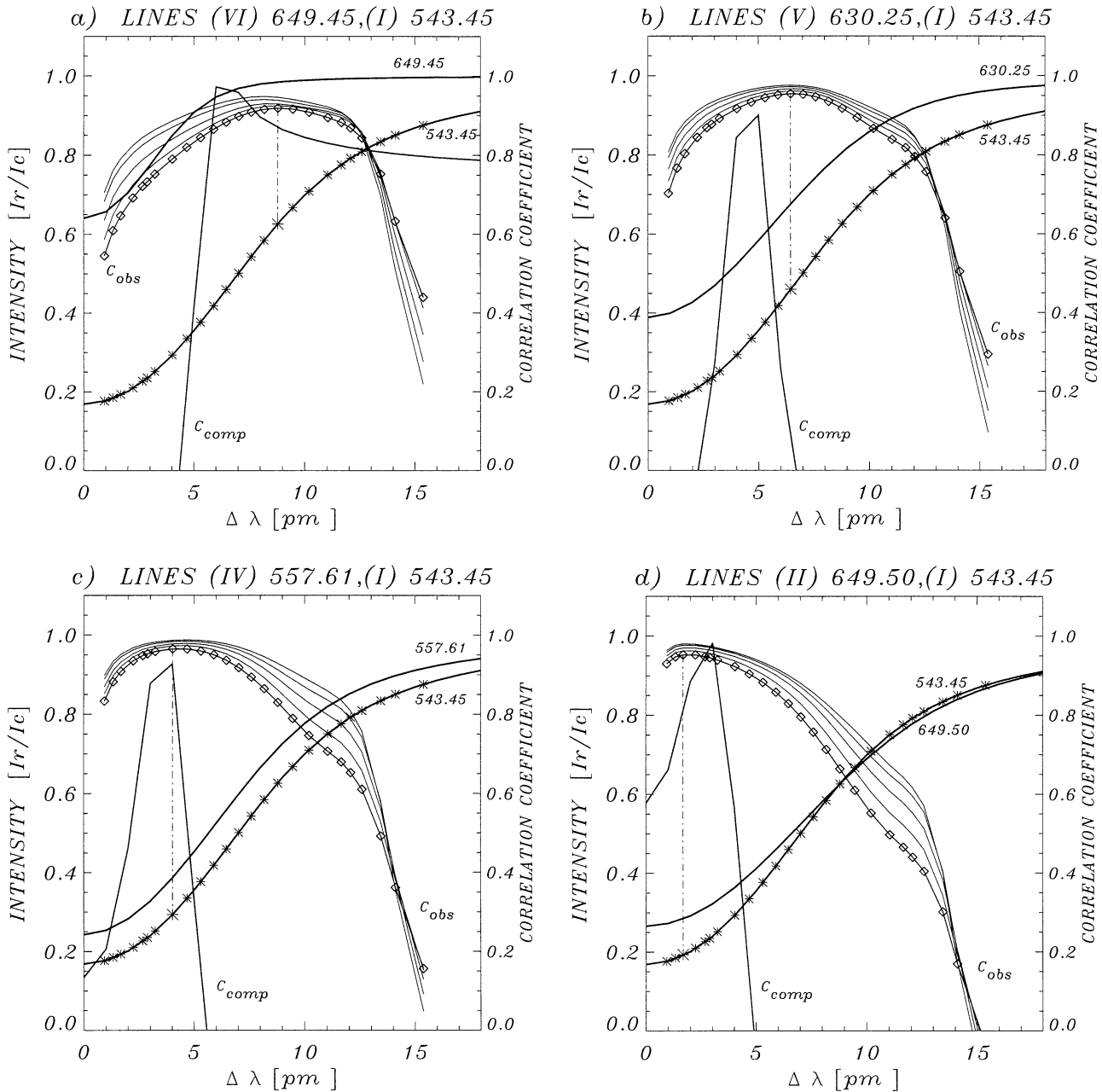


**Fig. 3a–d** Comparison of the experimental and theoretical correlation distributions. The symmetrized line profiles of pairs of spectral lines indicated on top of each panel **a** to **d** are given: VI,I; V,I; IV,I and II,I. The profiles are marked with their central wavelength. The  $c_i$  distribution =  $C_{obs}$  (diamonds) is given in each panel. The maximum of the distribution is indicated by a vertical dash-dotted line connected with the appropriate specific position in the profile of the second line. The other thin  $C_{obs}$  were obtained from spectra smoothed in the direction along the slit using of 5, 9, 15 and 21 points for averages. For details see Sect. 6. The full thin line marked as  $C_{comp}$  gives the  $k_i$  distribution resulted from the correlations of the computed LDCFs. For details see Sect. 5.

are shown in Fig. 4 and the heights of line formation are given in Table 2.

The observed granular and the intergranular mean profiles were composed only from scans placed in granules and in intergranular space, respectively. These profiles were compared with the theoretical ones resulting from the granular and the intergranular model. The agreement between the synthetic and observed profiles was optimized by varying the  $gf_\varepsilon$ -value and

the van der Waals factor. The macro- and microturbulence parameters are fixed to 1.6 km/s and 0.8 km/s, respectively. Unfortunately it was impossible to fit the VI-th line sufficiently with the same model used for the other five lines, perhaps due to uncertainties of the continuum in the observed spectra and/or due to blending by a water vapour line. The LDCFs were computed for every line profile in predefined displacements  $\Delta\lambda$  from -40 pm to +40 pm with respect to the line center at  $\lambda_0$ . The step

**Table 2.** Optical depths ( $\lg \tau_{500}$ ) of the positions of the maxima of the LDCF computed for the line centers for the granular (GR) and the intergranular (IG) model

line	I	II	III	IV	V	VI
GR	-4.20	-3.65	-2.95	-3.15	-2.50	-1.15
IG	-4.20	-3.55	-2.85	-3.05	-2.25	-1.10

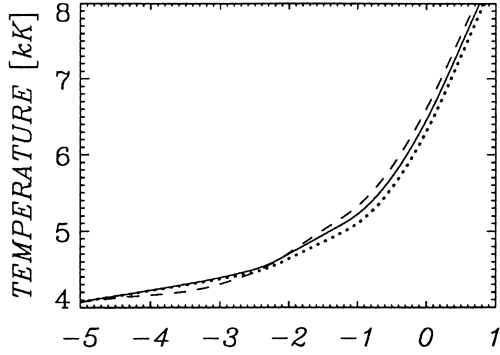


**Fig. 4.** Temperatures of the solar atmospheres used. The solid line is for T93-27, the dashed for the granular and the dotted for the intergranular model.

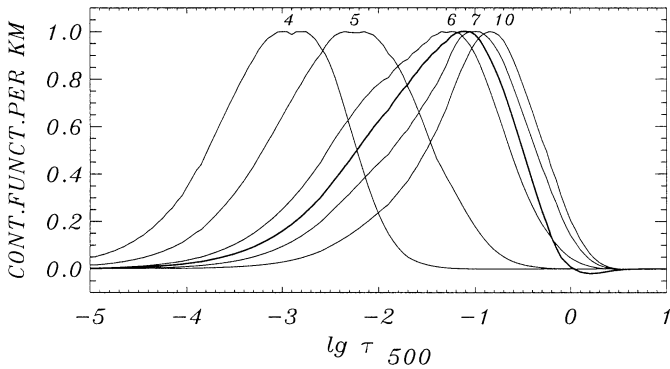


**Fig. 5.** Computed LDCFs for the line I (thin lines) and for line VI (thick line). The LDCFs 4,5,6,7 and 10 correspond to displacement  $\Delta\lambda = 4,5,6,7$  and  $10$  pm respectively. The thick line represents the LDCF computed for the line center of the line VI.

of  $\Delta\lambda$  was 1 pm. An example of several normalized LDCFs for line I (thin lines) together with the LDCF for the center of the line VI (thick line) is given in Fig. 5.

For every line pair, the LDCF corresponding to  $\lambda_o$  in the first line was correlated with LDCF corresponding to  $\lambda_o$  in the second line. An optical depth expressed in  $\lg \tau_{500}$  was used as an abscissa for the correlation. Thus we obtained the correlation coefficient  $k_0$ . The other correlation coefficients  $k_i$  ( $i=1,2,\dots,n$ ;  $n=40$  = number of predefined displacements  $\Delta\lambda$ ) resulted from correlations of the LDCF for the center of the first line with the LDCFs computed for  $n$   $\Delta\lambda$  displacements of the second line. One can recognize in Fig. 5, that there are very high correlations between the LDCF for  $i=6$  and 7, i.e.  $\Delta\lambda = 6$  and 7 pm, respectively, of line I (thin) and LDCF for the line center of line VI (thick). On the other hand we obtain a very low correlation

for the later LDCF (thick) with the LDCF for  $i=4$ , i.e.  $\Delta\lambda = 4$  pm of line I (thin). The distribution of the  $k_0, k_1, k_2, \dots, k_n$  we will call  $C_{comp}$ . In every pair of lines, the maximum of  $C_{comp}$  theoretically pointed out the corresponding  $\Delta\lambda$  in the wing of the second line, where the line depression is formed at the same height in the atmosphere as the center of the first line. The  $C_{comp}$  are shown in Fig. 3. Due to the finite  $\Delta\lambda$  spacing of 1 pm some curves peak below 1.0.

## 6. Discussion and conclusion

The experimental results show, that in all 15 possible pairs of the Fe I lines we have found high maxima of  $c_i$  distribution connected with a specific position in the wing of the second line. With increasing differences between the heights of formation of the lines, the maxima of  $c_i$  distributions tends to move more to the wing of the second line (panels c, b, and a of Fig. 3) with corresponding decreasing of the  $c_0$ .

These experimental results show that our method is applicable for all photospheric (even very weak) lines, but the results are better with medium strong lines. One should keep in mind, that also a magnetic field can affect the wings of the lines, except for the lines IV and I, which have a  $g_{eff}=0$  and are therefore not sensitive to the magnetic field. Thus the method is expected to work best for magnetically non-sensitive lines. A more important limitation is the necessity to obtain the spectra strictly simultaneously.

The theoretical  $k_i$  distributions reflect the behaviour of the experimental  $c_i$  distributions. Here we also recognize that with increasing differences between the heights of formation of the lines, the maxima of  $k_i$  distributions tends to move more to the wing of the second line with corresponding decreasing of the  $k_0$ . On the other hand the positions of all maxima of  $k_i$  distributions with respect to the  $c_i$  distributions are slightly shifted in direction to the centers of lines for 14 pairs of lines. An exception from this trend shows the pair of the purely velocity sensitive lines IV,I where the maxima of both distributions are at the same position (see Fig. 3, panel c). The shape of the  $k_i$  distributions are much narrower compared to the experimental  $c_i$  distributions. Probably important is here an observational effect caused by the limited spatial resolution. If the spatial resolution was better it would be possible to recognize every particular flow in the velocity field. It brings a more rapid decrease of the  $c_i$  distribution everywhere outside of the best correlation, which is connected with the appropriate height in the atmosphere. On the other hand, if the spatial resolution was worse, the maximum of the  $C_{obs}$  should get a flatter form. To simulate worse spatial resolution we have smoothed the spectra using different numbers of points for averages. The resulting  $c_i$  distributions from such smoothed spectra are shown in Fig. 3 with the full lines. As expected, the maxima become more flat and the  $c_i$  distributions are increasing mainly outside of the maxima. We can conclude, that:

- the described method to compare formation heights is suitable for photospheric lines and produces the best results for magnetically insensitive strong, but still unsaturated lines.

- the appearance of the maxima of  $c_i$  distributions in all 15 pairs supports the hypothesis of Grossmann-Doerth (1994), that it is possible to ascribe to a given position in the line profile a narrow height range, i.e. a point with limited resolution, in the atmosphere.
- spectra with higher spatial resolution result in more pronounced behaviour of the  $c_i$  distributions.
- our theoretical calculations of the LDCF are generally in agreement with the experimental results, in contrast to the statements of Sánchez et al. (1996), who investigated mainly the formation of polarization in a magnetic field. However, other advanced codes for theoretical calculations of line formation should be applied to prove our concept of comparing the FDVs from different positions in the profiles of two spectral lines.
- experimental results ( $c_i$  distributions) can be used as an additional sensitive criterion to distinguish between synthetic spectral profiles resulting from theoretical calculations.

*Acknowledgements.* We thank Dr. U. Grossmann-Doerth for the possibility to use his computer codes and for discussions and comments on a draft version of the paper. We thank Dr. H. Schleicher for helpful discussions and for his work on the KIS LIB routines. We thank an unknown referee for suggestions to improve the paper. The Vacuum Tower

Telescope is operated by the Kiepenheuer-Institut für Sonnenphysik, Freiburg, at the Observatorio del Teide of the Instituto de Astrofísica de Canarias. A.K. and J.R. thank for support of this work by grant GA SAV 4154/97.

## References

- Balthasar H., Grosser H., Schröter C., Wiehr E., 1990, A&A 235, 437  
 Beckers J.M., Milkey R.W., 1975, Solar Phys. 43, 289  
 Caccin B., Gomez M.T., Marmolino C., Severino G., 1977, A&A 54, 227  
 Espagnet O., Muller R., Roudier Th., Mein N., Mein P., 1995, A&AS 109, 79  
 Grossmann-Doerth U., 1994, A&A 283, 1018  
 Grossmann-Doerth U., Larsson B., Solanki S.K., 1988, A&A 204, 266  
 Gurtovenko E., Ratinikova V., de Jager C., 1974, Solar Phys. 37, 43  
 Holweger H., Müller E., 1974, Solar Phys. 39, 19  
 Kučera A., Rybák J., Wöhl H., 1995, A&A 298, 917  
 Makita M., 1977, Solar Phys. 51, 43  
 Magain P., 1986, A&A 163, 135  
 Mein P., 1971, Solar Phys. 20, 3  
 Sánchez Almeida J., Ruiz Cobo B., & del Toro Iniesta J.C., 1996, A&A 314, 295  
 Schleicher H., 1976, Thesis, University Göttingen